The study of the influence of heart ventricular wall thickness on pseudo-ECG

A. A. Razumov[*], K. S. Ushenin[*†], K. A. Butova[*], and O. E. Solovyova[*†]

Abstract — Electrocardiogram is a widespread method of diagnosis of heart diseases. Nevertheless, there are still issues related to connection of some physiological features of the myocardium with patterns observed on the electrocardiogram. In our work we studied the effect of ventricular remodelling, i.e., thickening of walls of ventricles typical for hypertrophic cardiomyopathy (HCM), on the pseudo-electrocardiogram on the surface of a volume conductor during myocardial activation from different sources. A model of two ventricles of the heart was developed for this purpose allowing us to vary ventricular geometry. The volume conductor surrounding the heart was a cubic homogeneous volume conductor. Simulation of a pseudo-electrocardiogram was performed by using a realistic ionic model of cardiomyocytes of the ventricles of the human heart and the bidomain model of the myocardium [15]. The zone of initial activation in the model was given on a part of the subendocardial surface or at one or two points corresponding to positions of electrodes of most common implantable devices. In the course of the study we revealed an inversion of the T-wave when changing the thickness of the left ventricle wall regardless of changes of properties of cardiomyocytes or myocardium conductivity. A linear dependence between the wall thickness of the left ventricle and peak amplitudes and integrals under QRS complex and T wave of the electrocardiogram was shown. We have qualitatively shown that with a change in the wall thickness of the left ventricle the pseudo-electrocardiogram changes stronger in the case of activation from one point than in activation from two points or activation of the entire subendocardium.

Keywords: mathematical physiology, pseudo-ECG, idealized ventricle model, ventricle wall thickness, bidomain model, numerical simulation, finite element method

MSC 2010: 92B99

Electrocardiogram (ECG) is a record of electrical potentials resulting from the heart activity. ECG is a non-invasive and affordable method of diagnosis of heart disease. Nevertheless, there are still questions about the connection of some physiological features of the myocardium with observed ECG patterns. Modern criteria for diagnosis of diseases using ECG assume that a physiological activation happens and thus are not suitable for cases of abnormal activation, for example, in the presence of artificial pacemakers or ectopic source.

[*]Ural Federal University, Ekaterinburg 620002

[†]Institute of Immunology and Physiology, Ural Branch of RAS, Ekaterinburg 620049. E-mail: konstantin.ushenin@urfu.ru

Computer simulation of myocardium can be used to estimate the impact of various physiological characteristics of the myocardium on ECG and pseudo-ECG, for example, inhomogeneities in ionic transmembrane currents [10], inhomogeneous electrical conductivity of the human torso as a volume conductor [9], in ischemic heart disease [18], as well as other factors [17].

In this paper we study the effect of thickening of the ventricular wall typical for hypertrophic cardiomyopathy (HCM) on pseudo-ECG on the surface of a volume conductor homogeneous in conductivity when activated from point sources corresponding to the position of electrode tipes of artificial pacemakers including devices of cardiac resynchronizing therapy.

For research we have developed an idealized geometric model of two ventricles of the heart surrounded by a conductive medium with variable parameters. Based on published data, we developed a series of 9 models with different thickness of the left ventricular (LV) wall. In order to simplify the processing of results, a cube with sides of 30 cm was taken as the volume conductor surrounding the heart [7,12]. The propagation of excitation wave in the myocardium was described by a bidomain model. Transmembrane currents were described by a realistic model of human heart ventricular cardiomyocytes [15]. The activation in the model was set on the LV subendocardial surface or at points in accordance with the location of electrodes of artificial pacemakers, including cardiac resynchronization therapy devices.

A significant influence of the thickness of LV wall on ECG characteristics is shown especially in single point stimulation of the myocardium.

1. Methods

1.1. Geometric model

The developed geometric model includes the left ventricle (LV) and right ventricle (RV) of the heart. Graphical primitives in the form of truncated ellipsoids were used to build the model similar to the model used in [2]. The model contains the following variable parameters: R_1 is the outer radius of LV, H is the length from the base to the apex of LV, d_{LV} is the thickness of LV wall at the base, d_{apex} is the thickness of the LV apex, A is the distance from the axis of LV to the most distant point of RV subepicardium at the base, d_{RV} is the RV wall thickness, (x_0, y_0) is the offset of the axis to build the subendocardium relative to the axis of subepicardium allowing us to specify the asymmetry of LV. In this model, the heights (H) of the LV and RV subendocardium apex coincide. This restriction sets a fixed thickness of the interventricular septum equal to the thickness of the LV free wall. All of these parameters are shown in Fig. 1. A more detailed description of the model is presented in Table 2.

The volume and mass of the left ventricle were calculated by the following formulas:

$$V_{LV} = \frac{4}{3}\pi(R_1 - d_{LV})^2(H - d_{apex}) \tag{1.1}$$

Table 1. Parameters for the series of geometric models.

No.	R_1, mm	d_{LV}, mm	d_{apex}, mm	d_{RV}, mm	A, mm	H, mm
	Normal anatomy (LV wall thickness is 6–10 mm)					
1.	38	7	7	4	69	76
2.	39	10	10	4	69	78
	Mild pathology (LV wall thickness is ¿ 10 mm)					
3.	40	13	13	4	69	79
4.	41	16	16	4	69	80
	Severe pathology (LV wall thickness is ¿ 19 mm)					
5.	42	19	19	4	69	81
6.	43	22	22	4	69	82
7.	44	25	25	4	69	83
8.	45	28	28	4	69	84
9.	46	31	31	4	69	85

$$m_{LV} = \rho \frac{4}{3}\pi(R_1^2 H - (R_1 - d_{LV})^2(H - d_{apex})) \tag{1.2}$$

where $\rho = 1.05$ g/m is the density of the myocardium [1].

In order to simplify the processing of results, the conductive medium model was a cube with sides of $30 \times 30 \times 30$ cm. Despite this assumption, the developed model repeats some of experimental papers [7, 12].

The pseudo-ECG was registered at 14 points on the cube. The points positioned at centers of cube sides are denoted according to the closest heart anatomic structures (APEX, BASE, ANTERIOR, RV, LV, POSTERIOR). Other registration points positioned at the cube vertices are denoted by (VX1-VX4, VX1'-VX4'). All points of pseudo-ECG registration are presented in Fig. 2b.

1.2. Models of normal and pathological anatomy

American Society of Echocardiography Guidelines [11] contain several criteria for diagnosis of heart ventricle diseases. The ranges of normal anatomy and anatomy for the mild and severe pathology are determined for each parameter. The four of all criteria presented in [11] directly describe geometric properties of heart ventricles, namely, the LV volume, LV mass, LV wall thickness, LV internal diameter.
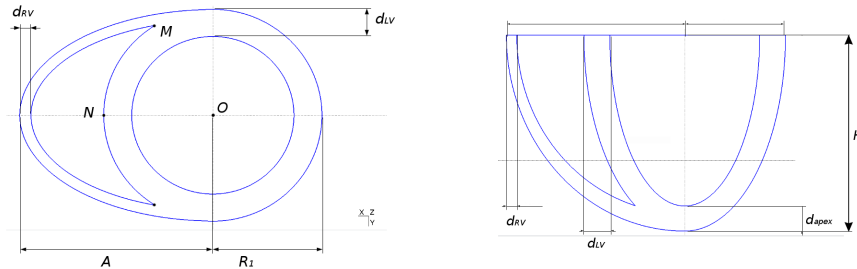
(a)   (b)

Figure 1. Cross-section at the base of ventricles (a) and longitudinal section of the model (b).
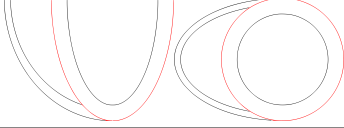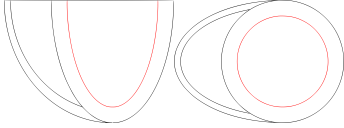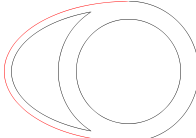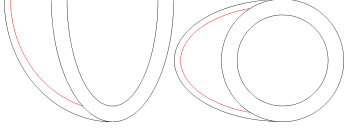
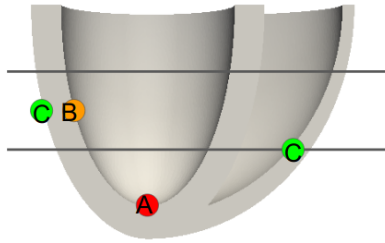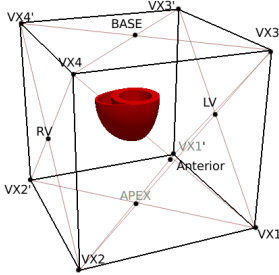**Table 2.** Description of geometry.

Surface	Equations
	$$\begin{cases} \dfrac{x^2}{R_1^2} + \dfrac{y^2}{R_1^2} + \dfrac{z^2}{H^2} = 1 \\ z \leqslant 0 \end{cases}$$
	$$\begin{cases} \dfrac{(x-x_0)^2}{(R_1 - d_{LV})^2} + \dfrac{(y-y_0)^2}{(R_1 - d_{LV})^2} + \dfrac{(z)^2}{(H - d_{apex})^2} = 1 \\ z \leqslant 0 \\ |x_0| < d_{LV} \\ |y_0| < d_{LV} \end{cases}$$
	$$\begin{cases} \dfrac{x^2}{A^2} + \dfrac{y^2}{R_1^2} + \dfrac{z^2}{H^2} = 1 \\ z \leqslant 0 \\ y \leqslant 0 \end{cases}$$
	$$\begin{cases} \dfrac{x^2}{(A - d_{RV})^2} + \dfrac{y^2}{(R_1 - d_{RV})^2} + \dfrac{z^2}{(H - d_{apex})^2} = 1 \\ \dfrac{x^2}{(A - d_{RV})^2} + \dfrac{y^2}{(R_1 - d_{RV})^2} + \dfrac{z^2}{(H - d_{apex})^2} \\ \geqslant \dfrac{x^2}{R_1^2} + \dfrac{y^2}{R_1^2} + \dfrac{z^2}{H^2} \\ z \leqslant 0 \\ y \leqslant 0 \end{cases}$$

(a)   (b)

Figure 2. Location of activation points in the model (a). Location of leads on the surface of the volume conductor for the qualitative analysis of ECG (b).
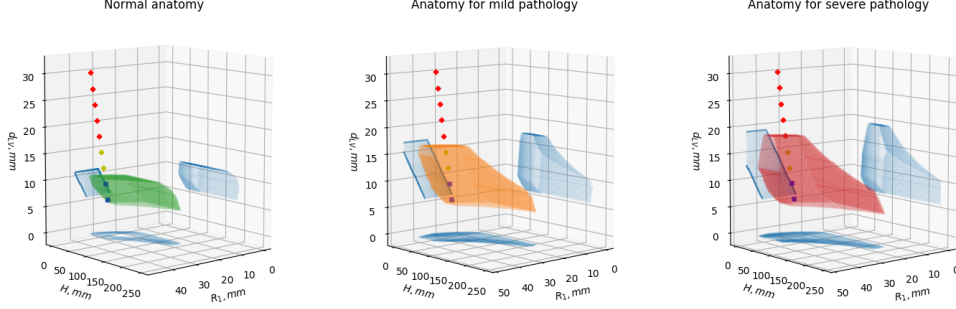
Figure 3. Space of model parameters (H, R_1, d_{LV}) and domains corresponding to the normal LV anatomy (left), small deviation from the normal state (center), and considerable deviation from the normal LV anatomy (right). Projections of these domains onto the corresponding coordinate planes are shown. The lower boundary is shown for the domain of severe pathology, i.e., the points lying outside of it correspond to the severe pathology. Dots indicate the parameters for the constructed series of models, i.e., blue points are for the normal anatomy, yellow points are for the mild pathology, red points are for the severe pathology.

Using formulas (1.1), (1.2), we obtained the ranges of LV height (H), LV diameter (R_1), and LV wall thickness (d_{LV}) determining the range of valid values for the normal anatomy, pathological anatomy, and severe pathological anatomy of LV for the developed geometric model. The visualization of such domains is presented in Fig.3.

Based on the parameters from [11], we have built a model of the heart ventricles anatomy for which all parameters are in the range of valid values for normal geometry. On the basis of this model, 8 more models with thicker walls were constructed. The increment of the thickness of LV walls was discrete and equal to P (P is the 'pathology' parameter). It was implemented by uniform increasing the LV radius R_1 by $P/3$, increasing d_{LV} and d_{apex} by P, and increasing the LV height by P. The parameters of all models are presented in Table 1 and visualized in Fig. 3.

1.3. The model of cardiac electrophysiology

In order to describe myocardial electrophysiology, a bidomain model [2] was used to describe the electrical potential φ_b in the passive conductor surrounding the myocardium, extracellular potential φ_e, and transmembrane potential $V_m \overset{\text{def}}{=} \varphi_i - \varphi_e$, where φ_i is the intracellular potential:

$$
\begin{cases}
\vec{\nabla} \cdot G_i(\vec{\nabla} V_m + \vec{\nabla} \varphi_e) = \beta_m(C_m \dfrac{\partial V_m}{\partial t} + i_{\text{ion}} + i_{\text{app}}) & \text{in } \Omega \times (0,T] \\
\vec{\nabla} \cdot ((G_i + G_e)\vec{\nabla}\varphi_e) = -\vec{\nabla} \cdot (G_i \vec{\nabla} V_m) & \text{in } \Omega \times (0,T] \\
\vec{\nabla} \cdot G_b \vec{\nabla}\varphi_b = 0 & \text{in } \Omega_b \times (0,T]
\end{cases}
\tag{1.3}
$$

where Ω is the domain of myocardium, Ω_b is the bath area around the myocardium, $T = 600\,\text{ms}$ is the duration of simulation, $C_m = 1\,\text{mF/cm}^2$ is the capacity of the membrane, $\beta_m = 1400\,\text{cm}^{-1}$ is the ratio of the membrane surface area to the

volume, $G_i = 12$ mS/cm, and $G_e = 45$ mS/cm are in this case the intracellular and extracellular diffusion coefficients in the myocardial region, and $G_b = 7$ mS/cm is the diffusion coefficient in the volume conductor [13].

The parameters G_e and G_i were chosen so that the duration of QRS-complex corresponds to the physiological one. The transmembrane currents i_{ion} were described by the ionic model of human ventricular cardiomyocytes TNNP 2006 [15].

In the present paper we do not take into account the anisotropy of the external environment and myocardium, and also its transmural heterogeneity.

The boundary conditions were specified so that there is no charge flow across the volume conductor ($\partial \varphi_b / \partial \mathbf{n} = 0$ on $\partial \Omega_b$) and there is no flow of charges from the intracellular medium into the volume conductor ($\partial \varphi_i / \partial \mathbf{n} = 0$ on $\partial \Omega$), and the charge flow from the extracellular medium is equal to the flow of charges in the domain of the volume conductor at each point of the surfaces ($G_e \partial \varphi_e / \partial \mathbf{n} = -G_b \partial \varphi_b / \partial \mathbf{n}$ on $\partial \Omega$). The potentials of the extracellular environment and the volume conductor are equal at each point on the torso-heart boundary ($\varphi_e = \varphi_b$ on $\partial \Omega$). The full mathematical formulation was given in [2].

The initial conditions were the following: $\varphi_e = 0$ in Ω and $\varphi_b = 0$ in Ω_b, $V_m = -86.709$ mV in Ω, and $i_{\mathrm{app}} = -50$ μA for 3 ms in the given domain of the myocardium for its activation. The following activation types were used to control the area of excitation: single point stimulation on subendocardial apex of the left ventricle (A); single-point stimulation on free wall subendocard of the left ventricle (B); simultaneous stimulation of two points corresponding to possible location of the electrode tips of the cardiac resynchronization therapy device (C); stimulation of 20% of LV subendocardial surface near the apex (S20); stimulation of the entire LV subendocardial surface (S100). The two latter variants simply simulate a realistic activation of the myocardium. The points for all activation options are shown in Fig. 2. The pseudo-ECG in the above leads (see Fig. 2) was calculated as the value of the extracellular potential φ_b at specified points.

The construction of model geometry and tetrahedral computational grid was performed with the use of Ani3D [4] and GMSH [6] packages. The model was calculated by the finite element method using the Oxford Chaste open source software [13].

The size of the rib element in the heart does not exceed 1.5 mm and 5 mm in the bath area. The computational grid for the heart with normal anatomy contained about 3117800 tetrahedrons and 539620 nodes. The ionic model was solved by the implicit Euler method with a constant step of 0.01 μs, the minimization was performed by Newton's method, the Jacobian was obtained in symbolic form from the ionic model. The calculations of the diffusion part used the step 0.05 μs. The numerical method was described in [3].

The formulation of the problem used here implies obtaining results for φ_e with the accuracy up to a constant. The default solver chose the solution vector with the minimal norm at each step. Thus, the whole solution was normalized and did not require introduction of a special point or Wilson's lead to normalize the results.

To test the influence of this approach on the results, we introduced additional
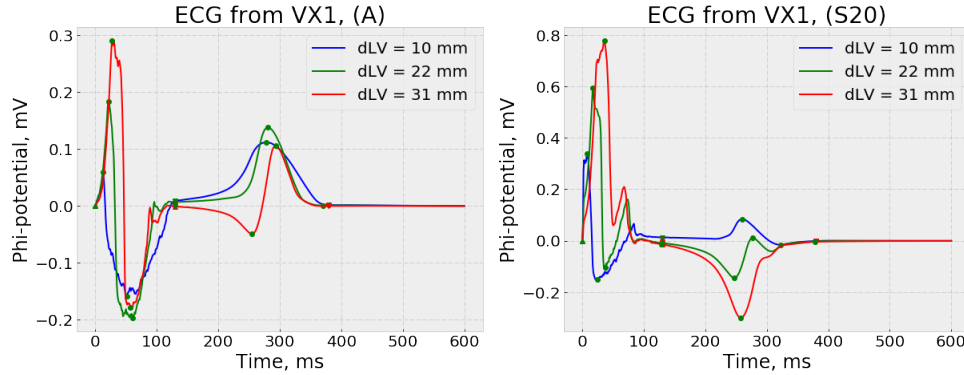
Figure 4. Pseudo-ECG signals in VX1 leads under activation (A) (left), in VX1 leads under activation (S20) (right) for different values of d_{LV}.
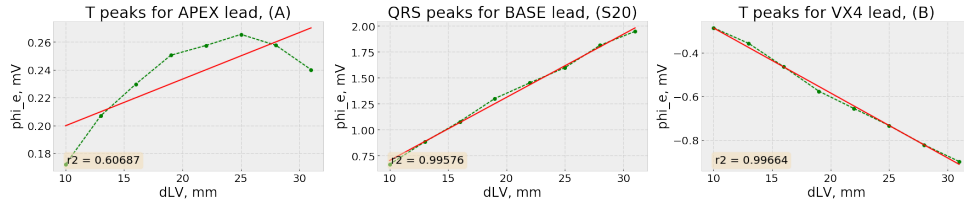

Figure 5. Examples of the dependence of ECG parameters on the thickness of the LV wall d_{LV}. Dotted line corresponds to ECG parameter values, solid line corresponds to linear regression model.

Wilson's leads at the points VX4, VX3, VX1 and RV, LV, APEX of the model. Such variants of normalization differ between themselves, but did not lead to a change in the results by more than 0.2 mV.

To analyze the correctness of the results, we refined the grid by splitting and recalculated the results of the reference model. The simulation results did not change more than by 7% for each time moment at each point. We believe that this accuracy is sufficient for the design of the experiment we have chosen.

2. Results

Considering nine constructed anatomical models of heart ventricles, we calculated pseudo-ECG and studied the dependence of pseudo-ECG on the surface of the volume conductor on the thickness of LV wall.

The qualitative analysis of the received pseudo-ECG signals from the above leads revealed that with increasing LV wall thickness (i.e., with increasing d_{LV}) the T-wave morphology becomes more complex in some leads, it becomes two-phase or even changes the direction to opposite to the orientation of the T-wave with normal LV geometry (see Figs. 4 and 11). For example, in the *VX1* lead, the T-wave for the normal anatomy is inverted with respect to the QRS complex and with increasing d_{LV} the T-wave transforms into a two-phase one (see Fig. 4, left). Similarly, for single-point activation (A) the T-wave changed its orientation in the lead VX2 for

the LV wall thickness 19 mm, in VX1 for 28 mm, and in APEX for 31 mm.

In addition, for increasing LV wall thickness we observed a linear dependence of the maxima of QRS-complex and T-wave on d_{LV} in many leads (see Fig. 4, left).

In order to study the dependence of maxima of QRS and T intervals and also the areas below them for all types of activation, we calculated the parameters of the pseudo-ECG at each point of the surface of volume conductor for each model, i.e., the peaks of the QRS-complex and T-wave and also the area under pseudo-ECG curves.

Further we studied the dependence of these values on the LV wall thickness d_{LV}. These dependences were approximated by the least squares method for each ith point of the surface using the linear model $y_i(d_{LV}) = k_i d_{LV} + b_i$, where y_i is the studied parameter of pseudo-ECG, d_{LV} is the LV wall thickness (see Fig. 5). Then we constructed the maps of parameters of linear regression, i.e., the maps of k_i, b_i and the maps of the determination coefficient R_i^2 (see Fig. 6) to estimate the quality of the linear dependence.

Positive slope values of k_i are observed for most models. That is, the increase of d_{LV} leads to the increase in the amplitude of signals (see Figs. 4 and 5). At the same time, for the single-point activation of myocardium (A) and (B), as well as for the activation of 20% of the LV subendocardial surface at the apical region (S20), the domain of maximal slopes k_i is located in the domain opposite to the activation zone (i.e., in the direction of the normal to the surface of the myocardium). And for two-point activation (C) and the activation of the entire LV subendocardial surface (S100) the maximal slopes k_i are located near the apex.

We revealed that for one-point activations (A) and (B) the dependence of maxima of QRS and T complexes can be assumed to be linear ($R_i^2 > 0.95$) only on the half of the conductor surface opposite to the activation point (see Fig. 6). For the areas under the QRS complex and T wave the dependence on the LV wall thickness d_{LV} cannot be explained by a linear model only on a small region of the conductor surface.

For all methods of activation of LV with more than one point of excitation (C), (S20), (S100) all parameters of pseudo-ECG can be described by a linear model because the values of the corresponding maps satisfy the inequality $R_i^2 > 0.95$ except for small areas of the surface close to the activation point. The only exception is the dependence of QRS maxima on LV wall thickness d_{LV} in the activation of the entire LV subendocardial surface (S100). In this case, on most of the surface of the volume conductor the value R_i^2 is close to zero (see Fig. 6 T–S100).

Further we studied the sensitivity of signals on the surface of the cube to changes in the LV wall thickness. To do this, we calculated deviations between pseudo-ECG signals at each point on the surface of the cube i for the normal heart $x_i(t)$ ($d_{LV} = 10$ mm) and the heart with the greatest degree of pathology $y_i(t)$ ($d_{LV} = 31$ mm) in the following way:

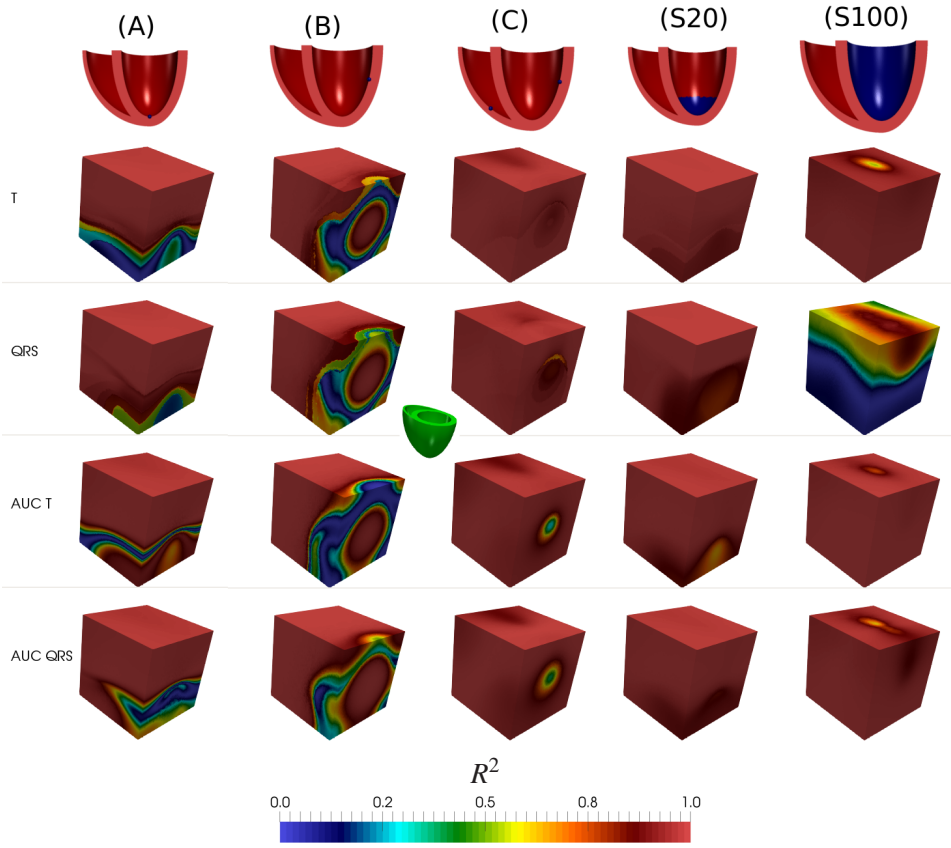$$\Delta_i = \int_{t=0}^{T} (x_i(t) - y_i(t))^2 dt \tag{2.1}$$

Figure 6. Maps of determination coefficient R^2 in linear regression of ECG parameters with respect to the ventricular wall thickness. The center part of the figure shows the orientation of ventricles in the cube. Here T and QRS denote the peaks of T-wave and QRS-complex; AUC T and AUC QRS are the areas under the T- and QRS-complex of pseudo-ECG.

and relative deviations as

$$\Delta_i^{\text{rel}} = \frac{\int_{t=0}^{T}(x_i(t) - y_i(t))^2 \mathrm{d}t}{\int_{t=0}^{T}(x_i(t))^2 \mathrm{d}t}. \tag{2.2}$$

The maps of deviations between signals of pseudo-ECG $(x_i(t), y_i(t))$ constructed by this method are presented in Fig. 7. Among all types of activations, the maximum absolute value 9.39 mV·ms of the difference of signals was achieved from the base in the lead APEX, and the maximal relative change is located in the lead ANTERIOR (see Fig. 7) and equals 15.3%. Such relative deviation of signals was primarily caused by low signal amplitudes in the case of normal ventricular anatomy (see Fig. 7b).

The following rule strictly holds for the model with ventricular activation from
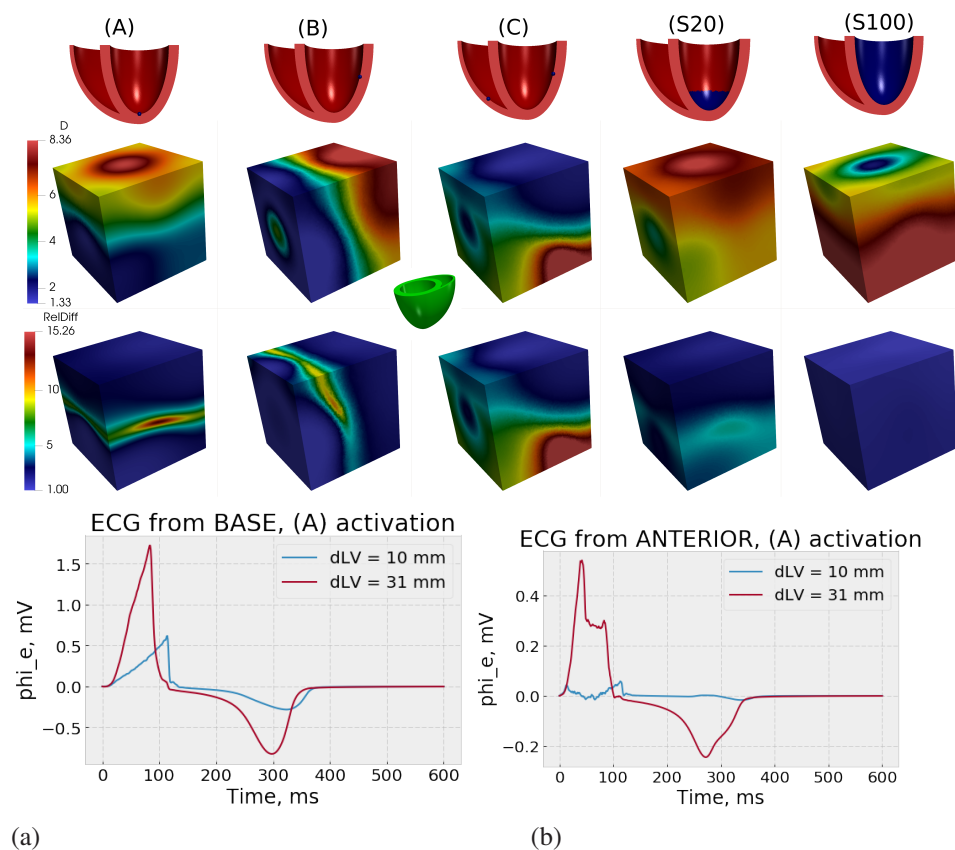
Figure 7. The differences in ECG on the surface of the volume conductor between the model with normal and the most pathological ventricular geometry. Top line shows the scheme of ventricular activations, middle lines present the maps of ECG difference and relative difference. Bottom left presents pseudo-ECG in BASE under activation (A). Bottom right presents pseudo-ECG in ANTERIOR under activation (A).

one point. For varying d_{LV} the strongest deviations of pseudo-ECG signal were observed on the side of the cube opposite to the LV activation point, and the signal at pathological changes of the thicknesses had the maximum amplitude compared to signals in other leads. At the same time, in comparison with other types of myocardial activation, the relative deviations between the recorded signal for normal anatomy and maximum pathological anatomy differed approximately twice.

3. Discussion

In the space of parameters of the geometric model corresponding to the normal anatomy of heart ventricles (see Fig. 3), there are ventricular models corresponding to the parameters (H, R_1, d_{LV}) with different volumes and masses of LV.

Thus, we have LV parameters ($H = 148$ mm, $R_1 = 21$ mm, $d_{LV} = 10$ mm) for

Figure 8. Maps of the extracellular potential φ_e for activation (A) at the time $t = 252$ ms in the section of the volume conductor. Left side is for $d_{LV} = 10$ mm, the center is for $d_{LV} = 31$ mm); right side is for pseudo-ECG signal in the VX1 lead for different d_{LV}.
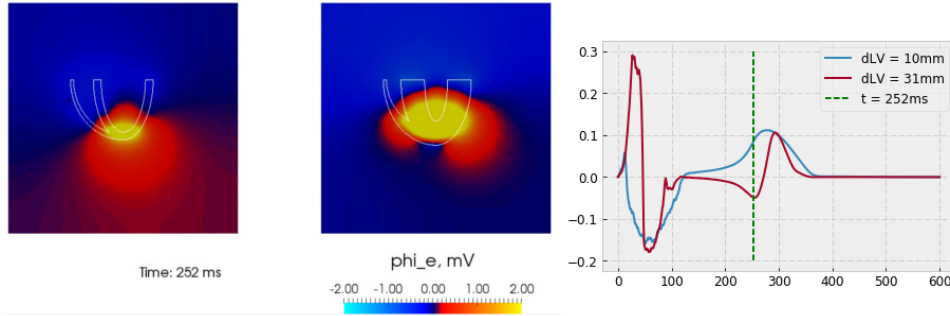

Figure 9. Maps of the extracellular potential φ_e for activation (S20) at the time $t = 257$ ms in the section of the volume conductor. Left side is for $d_{LV} = 10$ mm, the center is for $d_{LV} = 31$ mm); right side is for pseudo-ECG signals in the VX1 lead for different d_{LV}.
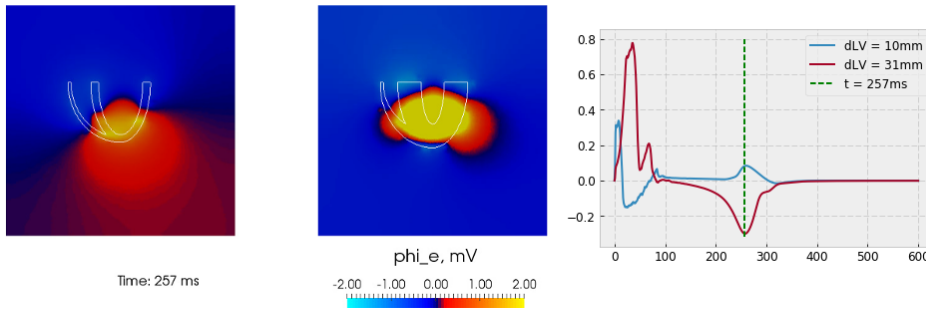
which the mass of ventricles is 177 g and the end-diastolic volume is 127 ml. For other LV parameters ($H = 140$ mm, $R_1 = 21$ mm, $d_{LV} = 6$ mm) the volume was 123 ml and the mass was 93 g. Thus, models with about the same volume of LV and with almost twice difference in mass of the myocardium may fall into one zone of acceptable values of parameters. We believe that such a situation is impossible in reality. Therefore, the zones of acceptable values should be substantially narrower if we take into account the criteria given in [11], for example, the ejection fraction, which cannot be taken into account in the geometric model.

Our results demonstrate the possibility of inversion of the T-wave with respect to the orientation of the T-wave at normal geometry of LV for point activations (A), (B) and activations (S20) (see Fig. 4 on the right, and Fig. 11). As is seen from Figs. 8 and 9, with thickening the LV wall the value of the extracellular potential φ_e near the apex at the time moment close to the peak of T-wave changes its sign to opposite. Thus, the T-wave changes its morphology in leads located near the apex. Changes in the anatomy of the heart are enough for this effect, and this does not require changes in properties of cardiomyocytes or in the conductivity of myocardial tissue.

We believe that the change in the direction of T-wave may relate to a change in
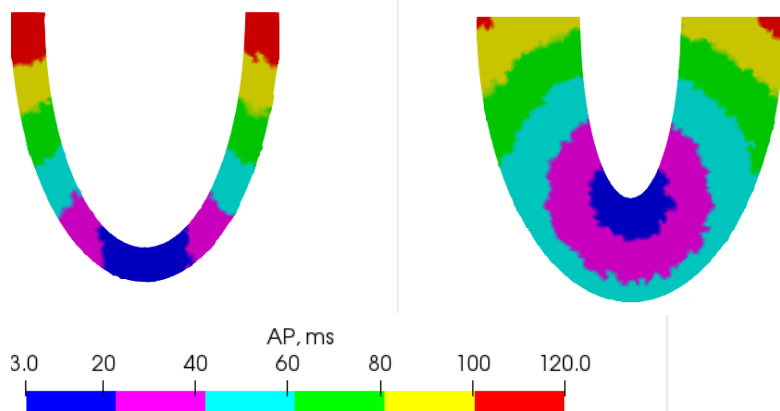
Activation map, $d_{LV} = 10\,\text{mm}$ Activation map, $d_{LV} = 31\,\text{mm}$

Figure 10. Activation maps at stimulation (A). Color scheme shows the arrival time of the excitation wave (i.e., the peak of depolarization).

the front of excitation wave propagation in LV walls when changing its geometry (see Fig. 10). So for normal geometry with point activation from the apex the wave front is close to a flat front and spreads from the apex to the base. When thickening LV walls, the wave front becomes spherical and the direction of the wave changes significantly near the top, which leads to a change in the morphology of pseudo-ECG in leads close to the apex of the heart.

Similar changes are observed in clinical practice. Under physiological activation, patients with the diagnosis of HCM demonstrate an inversion of the ECG T-wave in thoracic leads (see [5]). At the same time, both in clinical practice and models this effect is observed in leads close to the apex of the heart.

The analysis of maps of regression parameters for linear dependencies of ECG parameters on the thickness of LV wall shows that the electrocardiogram is most sensitive to geometric properties of ventricles in activation from a single point.

The observed effects can be used in the analysis of daily monitoring ECG data and setting up cardiac resynchronization therapy devices. Using the predicted linear dependence of ECG parameters on the thickness of LV walls within the framework of computer simulation, in case of deviation of clinical data from predictions of the model it is possible to pose a problem of identification of cellular remodelling parameters or variation of the myocardium conductivity parameter for an individual patient. To solve this problem, one can, for example, use ECG recorded during extrasystoles occurring in the course of daily monitoring. Extrasystoles are known to occur more often as the result of ectopic (point) stimulation, therefore, as the model predicts, are more sensitive to geometric parameters of the heart. To identify the properties of the myocardium for patients passing CRT, we can also use the data obtained by point stimulation used in the adjustment of the delay of ventricular electrodes stimulation. These problems will be solved in further studies of the possibility of diagnosis of the myocardium pathology with the aid of simulation.
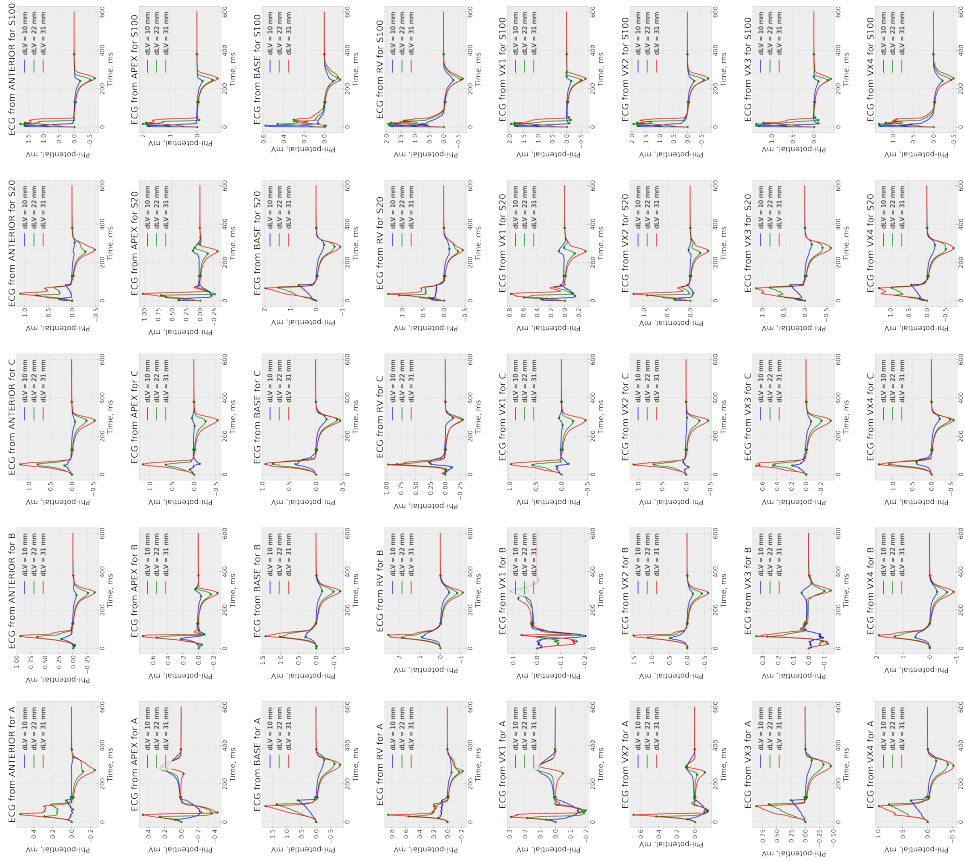
Figure 11. Pseudo-ECG signals from examined leads for different activation patterns.

The model developed here can be also used for analysis of experimental data and formulation of protocols of physiological research within the framework of a similar experimental model using a heart surrounded by a conductive medium. In particular, our model can be useful for studying electrophysiological properties of the myocardium of a hypertrophic heart or other cardiac abnormalities leading to geometric remodelling of the heart shape.

4. Limitations of the model

The analysis given at the moment does not include several important physiological features such as anisotropy of the myocardium, the myocardial heterogeneity in cardiomyocyte parameters, as well as a realistic volume conductor being inhomogeneous in conductivity, which the human torso is. In addition, known literature data do not describe quantitative variations of the listed parameters in the course of anatomical remodelling of the myocardium in hypertrophic cardiomyopathy. For small values of ECG amplitude the model used here may produce oscillations (see

Fig. 7b). The effect of oscillations of solutions is observed in many works on electro-cardiogram modelling [8, 9], some works demonstrate sharp additional peaks up to 0.1 mV in a neighbourhood of Q and S waves [14], and the works of both groups use different numerical methods. Despite all listed limitations of our model, we believe that all presented results will be qualitatively observed in more complex systems.

5. Conclusion

In this paper we presented an idealized geometric model of heart ventricles placed in a volume conductor in the form of a cube. Model parameters have been set according to medical literature. Using qualitative and statistical analysis, we studied the influence of ventricular wall thickness on the electrocardiogram on the surface of the volume conductor with several types of ventricular activation.

The study demonstrates an inversion of the T-wave due to changes in the LV geometry regardless of changes in the properties of cardiomyocytes or myocardial conductivity. A linear dependence between ECG parameters and LV wall thickness is shown. A higher sensitivity of ECG to changes in LV wall thickness in the case of ventricular activation from one point than the in activation from two points or activation of the entire subendocardium is also shown.

In our opinion, the simulation results partially explain the inversion phenomenon of T-waves in hypertrophic cardiomyopathy. The obtained regularities can be used to develop new criteria for diagnosis of HCM, and also to help with development of algorithms for processing the results of daily ECG monitoring and algorithms for adjusting cardiac resynchronization therapy devices.

References

1. AD Annexes, *Annals of the ICRP* **39** (2009), 47–70.

2. M. Boulakia, S. Cazeau, M. A. Fernández, J.-F. Gerbeau, and N. Zemzemi, Mathematical modelling of electrocardiograms: a numerical study. *Annals Biomed. Engrg.* **38** (2010), 1071–1097.

3. Chaste Project, *Chaste: Finite Element Implementations*. https://chaste.cs.ox.ac.uk/chaste /tutorials/release_2.3/ChasteGuides/FiniteElementImplementations/fem_implementation.pdf, 2011.

4. A. A. Danilov, Unstructured tetrahedral mesh generation technology, *Comp. Math. Math. Phys.* **50** (2010), 139–156.

5. A. S. Flett, V. Maestrini, D. Milliken, M. Fontana, T. A. Treibel, R. Harb, D. M. Sado, G. Quarta, A. Herrey, J. Sneddon, P. Elliot, W. McKenna, and J. C. Moon, Diagnosis of apical hypertrophic cardiomyopathy: T-wave inversion and relative but not absolute apical left ventricular hypertrophy. *Int. J. Cardiology* **183** (2015), 143–148.

6. C. Geuzaine and J.-F. Remacle, Gmsh: A 3-D finite element mesh generator with built-in pre-and post-processing facilities. *Int. J. Numer. Methods Engrg.* **79** (2009), 1309–1331.

7. L. S. Green, B. Taccardi, P. R. Ershler, and R. L. Lux, Epicardial potential mapping. Effects of conducting media on isopotential and isochrone distributions. *Circulation* **84** (1991), 2513–2521.

8. D. U. J. Keller, R. Kalayciyan, O. Dössel, and G. Seemann, Fast creation of endocardial stimu-

lation profiles for the realistic simulation of body surface ECGs. In: *World Congress on Medical Physics and Biomedical Engineering, September 7–12, 2009, Munich, Germany*, 2009, 145–148.

9. D. U. J. Keller, F. M. Weber, G. Seemann, and O. Dossel, Ranking the influence of tissue conductivities on forward-calculated ECGs. *IEEE Trans. Biomed. Engrg.* **57** (2010), 1568–1576.

10. D. U. J. Keller, D. L. Weiss, O. Dossel, and G. Seemann, Influence of I_{Ks} heterogeneities on the genesis of the T-wave: a computational evaluation, *IEEE Trans. Biomed. Engrg.* (2012) **59**, 311–322.

11. R. M. Lang, M. Bierig, R. B. Devereux, F. A. Flachskampf, E. Foster, P. A. Pellikka, M. H. Picard, M. J. Roman, J. Seward, J. S. Shanewise et al., Recommendations for chamber quantification: a report from the American Society of Echocardiography Guidelines and Standards Committee and the Chamber Quantification Writing Group, developed in conjunction with the European Association of Echocardiography, a branch of the European Society of Cardiology. *J. Amer. Soc. Echocardiography* **18** (2005), 1440–1463.

12. R. S. MacLeod, B. Taccardi, and R.L. Lux, The influence of torso inhomogeneities on epicardial potentials. In: *Computers in Cardiology 1994*, IEEE, 1994, pp. 793–796.

13. G. R. Mirams, C. J. Arthurs, M. O. Bernabeu, R. Bordas, J. Cooper, A. Corrias, Y. Davit, S.-J. Dunn, A. G. Fletcher, D. G. Harvey et al., Chaste: an open source C++ library for computational physiology and biology. *PLoS Computational Biology* **9** (2013), e1002970.

14. E. Schenone, A. Collin, and J.-F. Gerbeau, Numerical simulation of electrocardiograms for full cardiac cycles in healthy and pathological conditions. *Int. J. Numer. Meth. Biomed. Engrg.* **32** (2016), No. 5, e02744.

15. K. H. W. J. Ten Tusscher and A. V. Panfilov, Alternans and spiral breakup in a human ventricular tissue model. *Amer. J. Physiology-Heart and Circulatory Physiology* **291** (2006), H1088–H1100.

16. L. Tung, *A bi-domain model for describing ischemic myocardial dc potentials*. Ph.D. Thesis, Massachusetts Institute of Technology, 1978.

17. K. S. Ushenin, A. Dokuchaev, S. M. Magomedova, O. V. Sopov, V. V. Kalinin, and O. Solovyova, *Role of Myocardial Properties and Pacing Lead Location on ECG in Personalized Paced Heart Models*, IEEE, 2017.

18. M. Wilhelms, O. Dossel, and G. Seemann, In silico investigation of electrically silent acute cardiac ischemia in the human ventricles. *IEEE Trans. Biomed. Engrg.* **58** (2011), 2961–2964.